

LA-UR-21-23745

Approved for public release; distribution is unlimited.

Title: Green function approach to R-matrix theory and applications to light nuclear reactions

Author(s): Paris, Mark W.

Intended for: University of Notre Dame, Dept. of Physics, Nuclear Physics Seminar

Issued: 2021-04-20 (rev.1)

Disclaimer:

Los Alamos National Laboratory, an affirmative action/equal opportunity employer, is operated by Triad National Security, LLC for the National Nuclear Security Administration of U.S. Department of Energy under contract 89233218CNA000001. By approving this article, the publisher recognizes that the U.S. Government retains nonexclusive, royalty-free license to publish or reproduce the published form of this contribution, or to allow others to do so, for U.S. Government purposes. Los Alamos National Laboratory requests that the publisher identify this article as work performed under the auspices of the U.S. Department of Energy. Los Alamos National Laboratory strongly supports academic freedom and a researcher's right to publish; as an institution, however, the Laboratory does not endorse the viewpoint of a publication or guarantee its technical correctness.



Green function approach to R-matrix theory and applications to light nuclear reactions

Mark Paris

Theoretical Division

Nuclear & Particle Physics, Astrophysics & Cosmology (T-2)

Univ. Notre Dame, Dept. of Physics

Nuclear Physics seminar

2021-04-19

LA-UR-21-23745

Outline

1. Introduction & Motivation

2. Theory & Formalism

- Scattering theory
- Green functions
- R-matrix in Green-Bloch formulation

3. Evaluations

- NN
- ^5Li
- ^{10}Be

4. Conclusion & Outlook



Introduction

- Who: Light-element nuclear data evaluation "team" @ LANL/Theoretical Div.
 - Gerry Hale & MP
 - LANL collaborators
 - *D. Dodder, K. Witte, A. Sierk, R. MacFarlane, N. Gibson, W. Haeck*
 - External collaborators
 - D.Brown(BNL), C.Brune(OU), J.deBoer(ND), R.Capote(IAEA), V.Dimitriou(IAEA), I.Thompson(LLNL) & *many others*
- What: Light-element cross section evaluation for science and applications
- When: 70's → current
- Why...motivations, next slides



Motivation I

Theoretical

Address *open* problem of relativistic, multichannel scattering/reactions of composite strongly interacting (QCD) *objects* (*a.k.a.*, *nuclei*)

1. Elementary Particle Theory of Composite Particles*

STEVEN WEINBERG†

Department of Physics, University of California, Berkeley, California

(Received 13 November 1962)

THIS is the first of a series of articles, in which we hope to develop a method for the calculation of strong interaction processes.

2. Quasiparticles and the Born Series*

THIS is the second of a series of papers, in which we hope to develop a practicable method of calculating strong interaction processes.

3. Systematic Solution of Multiparticle Scattering Problems*

THIS is the third paper in our current series on the quasiparticle method. The first¹ showed how fi-

4. ??? The 4th paper never appears

In the fourth paper we will extend these ideas to the fully relativistic case.¹ Here we shall see that the quasiparticles can provide the force that makes their introduction a necessity.

- **Phenomenological R-matrix parametrization** of light-element scattering/reactions (largely non-relativistic) may give clues about the more general problem



Motivation II

Practical Applications

Continuous (and multi-group) representation of scattering/reaction data is important for a variety of applications

- Nuclear astrophysics & cosmology
- Neutrinos and fundamental symmetries
- Energy
- Nuclear criticality & safety
- Nuclear security



LANL light-element program

- All compound systems A<20 (and a few above)
- Recent work in 2020:

Projectile\Target	¹ H	² H	³ H	³ He	⁴ He	⁶ Li	⁷ Li
<i>n</i>	2020	VIII.0	VIII.0	VIII.0	VIII.0	2020	VIII.0
<i>p</i>	2020	VIII.0	VIII.0	VIII.0	2020	VIII.0	VIII.0
<i>d</i>		VIII.0	VIII.0	2020	VIII.0 ^a	VIII.0	VIII.0
<i>t</i>			VIII.0	VIII.0	2020	VIII.0	TENDL09
<i>h</i> (³ He)				VIII.0	VIII.0	VIII.0	TENDL09
α					VIII.0	TENDL09	TENDL09
¹¹ B ($\alpha+{^7\text{Li}}$, $\alpha+{^7\text{Li}}^*$, t+ ⁸ Be, n+ ¹⁰ B); ¹¹ C ($\alpha+{^7\text{Be}}$, p+ ¹⁰ B)							
¹² C ($\alpha+{^8\text{Be}}$, p+ ¹¹ B)							
¹³ C (n+ ¹² C, n+ ¹² C*)							
¹⁴ C (n+ ¹³ C)							
¹⁵ N (p+ ¹⁴ C, n+ ¹⁴ N, $\alpha+{^{11}\text{B}}$)							
¹⁶ O (g+ ¹⁶ O, $\alpha+{^{12}\text{C}}$)							
¹⁷ O (n+ ¹⁶ O, $\alpha+{^{13}\text{C}}$)							
¹⁸ Ne (p+ ¹⁷ F, p+ ¹⁷ F*, $\alpha+{^{14}\text{O}}$)							



Theory

Overview of R-matrix approach

- I. Solve the Schrodinger equation for the **scattering** problem

(by imposition of scattering *Boundary Conditions* – see next slide)

- II. But rather than **match** the data at macroscopically large distances from the scatterer

(as is usually done)

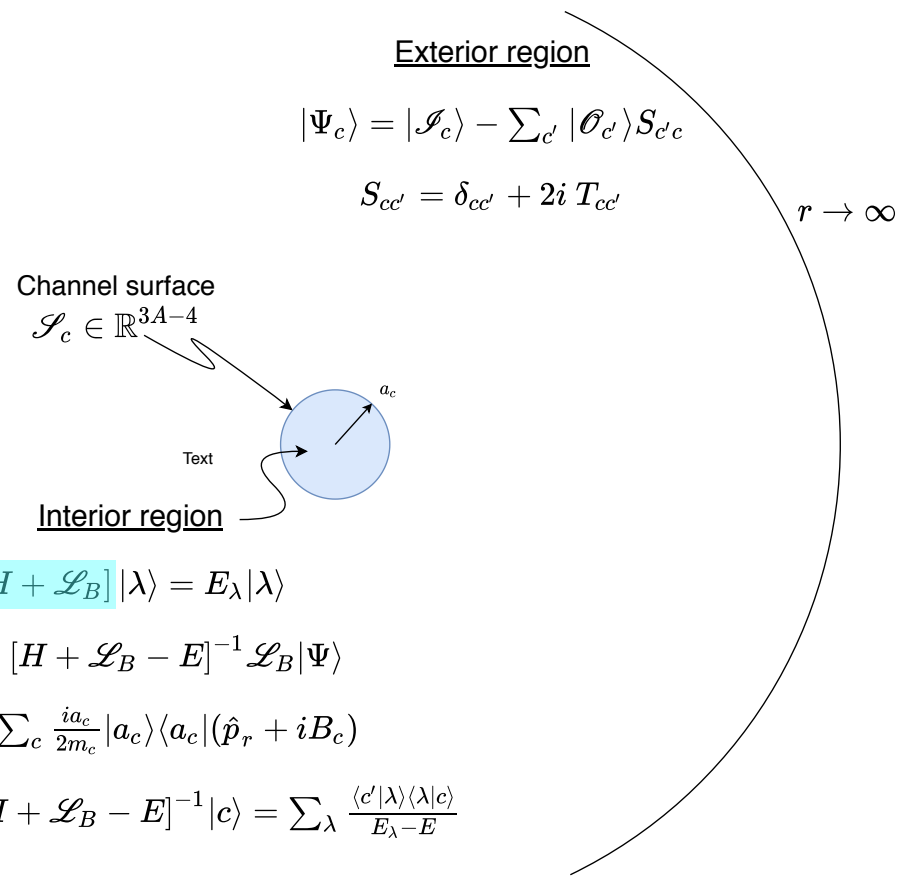
- III. We assume that the asymptotic wave function is known down to microscopic scales

(Coulomb or free)

- IV. **Match** at a finite radius – the **channel radius**: r_c or a_c

- V. Why?

The finite channel surface boundary between *Interior* & *Exterior* regions allows the definition of a **compact, Hermitian operator**



$$[H + \mathcal{L}_B] |\lambda\rangle = E_\lambda |\lambda\rangle$$

$$|\Psi\rangle = [H + \mathcal{L}_B - E]^{-1} \mathcal{L}_B |\Psi\rangle$$

$$\mathcal{L}_B = \sum_c \frac{ia_c}{2m_c} |a_c\rangle \langle a_c| (\hat{p}_r + iB_c)$$

$$R_{B,c'c} = \langle c' | [H + \mathcal{L}_B - E]^{-1} | c \rangle = \sum_\lambda \frac{\langle c' | \lambda \rangle \langle \lambda | c \rangle}{E_\lambda - E}$$

Compound system & channels

- ${}^5\text{Li}$ – interior region
- $\text{p}+{}^4\text{He}$, $\text{d}+{}^3\text{He}$, ... – exterior, asymptotic region



Theory

Scattering: Boundary condition

- Solve the Schrodinger equation for $E>0$, in the continuum

$$\left\{ -\frac{\hbar^2}{2\mu} \nabla^2 + V(\mathbf{r}) \right\} \Psi(\mathbf{r}) = E\Psi(\mathbf{r})$$

- Boundary condition

- Suppose

$$\Psi(\mathbf{r}) = \int \frac{d^3k'}{(2\pi)^{3/2}} e^{i\mathbf{k}' \cdot \mathbf{r}} \Psi(\mathbf{k}') \implies \lim_{|\mathbf{r}| \rightarrow \infty} \Psi(\mathbf{r}) \rightarrow 0 \text{ (by Riemann-Lebesgue)}$$

- Correct BC for incoming plane wave with \mathbf{k}

$$\Psi(\mathbf{r}) = \int \frac{d^3k'}{(2\pi)^{3/2}} e^{i\mathbf{k}' \cdot \mathbf{r}} \Psi(\mathbf{k}') + e^{i\mathbf{k} \cdot \mathbf{r}}$$

only remaining term
as $|\mathbf{r}| \rightarrow \infty$

- Energy conservation [assume $\ell=0$, elastic only]

$$\lim_{|\mathbf{r}| \rightarrow \infty} \Psi(\mathbf{r}) \rightarrow \underbrace{\frac{e^{-ikr}}{r}}_{\text{Incoming wave}} - \underbrace{\frac{e^{+ikr}}{r}}_{\text{Outgoing wave}} S_{\ell=0}(k)$$

Scattering "matrix"

Phase shift

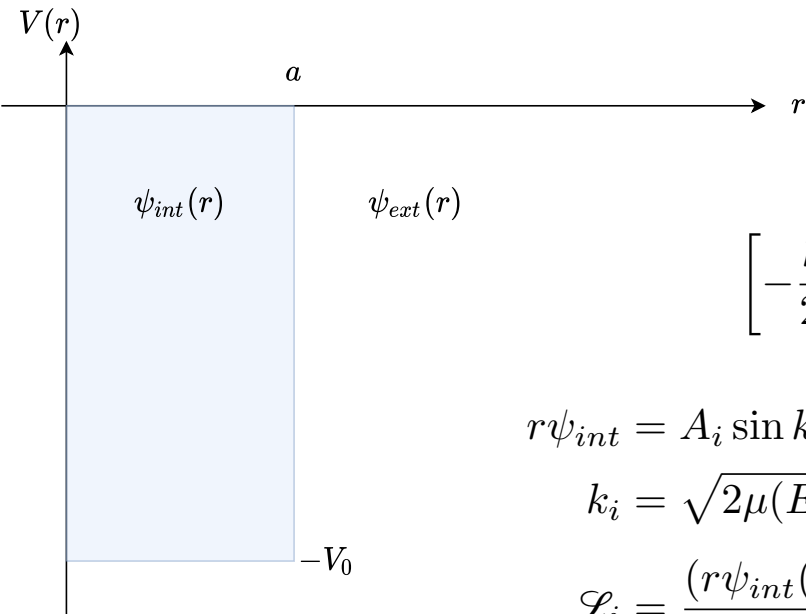
$$S_{\ell=0}(k) = e^{2i\delta_0(k)}$$



Theory

Scattering: Matching example [finite square well; $\ell=0$]

- Finite square well



$$\left[-\frac{\hbar^2}{2\mu} (r\psi(r))'' + V(r) \right] (r\psi(r)) = E(r\psi(r))$$

$$r\psi_{int} = A_i \sin k_i r$$

$$k_i = \sqrt{2\mu(E + V_0)}$$

$$\mathcal{L}_i = \left. \frac{(r\psi_{int}(r))'}{r\psi_{int}(r)} \right|_{r=a}$$

$$r\psi_{ext} = A_e \sin(k_e r + \delta_0(E))$$

$$k_e = \sqrt{2\mu E}$$

$$\mathcal{L}_e = \left. \frac{(r\psi_{ext}(r))'}{r\psi_{ext}(r)} \right|_{r=a}$$

Matching condition at $r=a$: $\mathcal{L}_i = \mathcal{L}_e$

- Logarithmic derivative continuity

$$k_i^{-1} \tan k_i a = k_e^{-1} \tan(k_e a + \delta_0)$$

Caveat: unlike here, R-matrix matching occurs anywhere outside the range of the strong interaction



Theory

Green functions

- Usual application to inhomogeneous differential equations

- Such as the Poisson equation EM
- The Green function (or operator) is the *inverse* of the differential operator:

$$\boxed{\text{“}G = -(\nabla^2)^{-1}\text{”} \longleftrightarrow -\nabla'^2 G(\mathbf{r}') = 4\pi\delta(\mathbf{r}')}}$$

$$\begin{aligned} -\nabla^2 \phi(\mathbf{r}) &= 4\pi\rho(\mathbf{r}) \\ \phi(\mathbf{r}) &= \int d^3 r' \frac{1}{|\mathbf{r} - \mathbf{r}'|} \rho(\mathbf{r}') \end{aligned}$$

- R-matrix approach requires *generalized* Green function

- Incorporate *boundary condition* information directly into Green function

$$(H + \hat{\mathcal{L}}_a^{(0)} - E) |\Psi\rangle = |F\rangle$$

$$|F\rangle = |f\rangle + A|a\rangle$$

$$\hat{\mathcal{L}}_a^{(0)} = \frac{i\hbar}{2\mu} |a\rangle\langle a| \hat{p}_r$$

$$\langle r | \hat{p}_r = \frac{-i}{r} \frac{\partial}{\partial r} r \langle r |$$

$$\boxed{(H(r) + \hat{\mathcal{L}}_a^{(0)}(r) - E) \Psi(r) = F(r)}$$

$$F(r) = f(r) + A \frac{\delta(r-a)}{r^2}$$

$$\hat{\mathcal{L}}_a^{(0)}(r) = \frac{\hbar^2}{2ma} \frac{\delta(r-a)}{r^2} \frac{d}{r} r$$

$$\int_{a-\epsilon}^{a+\epsilon} dr$$

$$(H(r) - E) \Psi(r) = f(r)$$

$$\left. \frac{\hbar^2}{2\mu a} \frac{d}{dr} (r\Psi(r)) \right|_{r=a} = A$$

$$\forall r$$

$$r = a$$



Theory

R-matrix: Exterior & Interior region wave functions

Exterior region

$$[H_E - E] |\mathcal{E}_c\rangle = 0$$

$$\mathcal{E}_c = \mathcal{O}_c \text{ or } \mathcal{I}_c$$

$$|\Psi_c\rangle = |\mathcal{I}_c\rangle - \sum_{c'} |\mathcal{O}_{c'}\rangle S_{c'c}$$

Channel surface

$$\mathcal{S}_c \in \mathbb{R}^{3A-4}$$

Interior region

$$\mathcal{H}_I(a_c, b_c) |\lambda(a_c, b_c)\rangle = E_\lambda(a_c, b_c) |\lambda(a_c, b_c)\rangle$$

$$\mathcal{H}_I(a_c, b_c) = H_I + \mathcal{L}_b(a_c)$$

$$\mathcal{L}_b(a_c) = \sum_c |a_c; c\rangle \langle a_c; c| \frac{ia_c^2}{2\mu_c} (\hat{p}_r + ib_c)$$

$$r \rightarrow \infty$$



Theory

Bloch-Green formalism

- Solve the multichannel, scattering (Schrodinger) equation

$$(H - E) |\Psi_c\rangle = 0$$

$$\mathcal{H}_I(a_c, b_c) |\lambda(a_c, b_c)\rangle = E_\lambda(a_c, b_c) |\lambda(a_c, b_c)\rangle$$

$$(H + \hat{\mathcal{L}}_b - E) |\Psi_c\rangle = \hat{\mathcal{L}}_b |\Psi_c\rangle$$

$$\mathcal{H}_I(a_c, b_c) = H_I + \hat{\mathcal{L}}_b(a_c)$$

$$G_b = (H + \hat{\mathcal{L}}_b - E)^{-1}$$

$$\hat{\mathcal{L}}_b(a_c) = \sum_c |a_c; c\rangle \langle a_c; c| \frac{ia_c^2}{2\mu_c} (\hat{p}_r + ib_c)$$

$$|\Psi_c\rangle = G_b \hat{\mathcal{L}}_b |\Psi_c\rangle$$

$$|a_c; c\rangle = |a_c; j_c m_c; \ell_c s_c\rangle \langle a_c; j_c m_c; \ell_c s_c|$$

- Matching @ $r_c = a_c$:

$$|\Psi_c\rangle = G_b \hat{\mathcal{L}}_b |\Psi_c\rangle$$

$$|\Psi_c\rangle = |\mathcal{I}\rangle_c - \sum_{c'} |\mathcal{O}\rangle_{c'} S_{c'c}$$

$$|\mathcal{I}\rangle - |\mathcal{O}\rangle S = G_b(a_c)(\mathcal{D} - b) \{|\mathcal{I}\rangle - |\mathcal{O}\rangle S\} \quad \leftarrow \text{Matching at } a_c$$

- Definition of **R-matrix** and **S-matrix**

$$\begin{aligned} G_{b;c',c} &= \langle c' | (H + \hat{\mathcal{L}}_b - E)^{-1} | c \rangle \\ &= \sum_{\lambda} \langle c' | (H + \hat{\mathcal{L}}_b - E)^{-1} | \lambda \rangle \langle \lambda | c \rangle \\ &= \sum \frac{\langle c' | \lambda \rangle \langle \lambda | c \rangle}{E_{\lambda} - E} \quad \leftarrow \text{Spectral representation} \end{aligned}$$



$$R(a_c, b_c) = \sum_{\lambda} \frac{\gamma_{\lambda, c'} \gamma_{\lambda, c}}{E_{\lambda} - E} \quad \gamma_{\lambda, c} = \frac{a_c}{\sqrt{2\mu_c}} \langle \lambda | c \rangle \in \mathbb{R}$$

NB : S matrix does not depend on a_c, b_c

$$\begin{aligned} S &= O^{-1} I + 2iO^{-1} R_L O^{-1} \\ R_L &= [1 + R(B - L)]^{-1} R \end{aligned}$$

$$L \leftrightarrow L_{c'c} = \delta_{c'c} L_c$$

$$B \leftrightarrow B_{c'c} = \delta_{c'c} b_c$$

$$L_c = \frac{a_c}{O_c} \frac{\partial O_c}{\partial r_c} \Big|_{r_c=a_c}$$

Theory

Bloch-Green formalism: S-matrix unitarity

$$S = O^{-1}I + 2iO^{-1}R_L O^{-1}$$

$$R_L^{-1} = R^{-1} + B - L$$

$S^\dagger S = 1$ Unitary constraint

$$\begin{aligned} &= 1 + 2iI^{-1}R_L^\dagger \left[(R_L^\dagger)^{-1} - R_L^{-1} - 2iI^{-1}O^{-1} \right] R_L O^{-1} \\ &= 1 + 4I^{-1}R_L^\dagger \left[\underbrace{\text{Im } B}_{\rightarrow 0} - \underbrace{\text{Im } L + I^{-1}O^{-1}}_{\rightarrow 0, \Rightarrow P = \text{Im } L = (F^2 + G^2)^{-1}} \right] R_L O^{-1} \end{aligned}$$

- Unitarity requires B real
- Energy independent level E_λ and reduced width $\gamma_{c\lambda}$ require B constant
- Unitarity is preserved for finite set $\{E_\lambda, \gamma_{c\lambda}\}$



Unitarity implications

$$\left. \begin{array}{lcl} \delta_{fi} & = & \sum_n S_{fn}^\dagger S_{ni} \\ S_{fi} & = & \delta_{fi} + 2i\rho_f T_{fi} \\ \rho_n & = & \delta(H_0 - E_n) \end{array} \right\} \quad T_{fi} - T_{fi}^\dagger = 2i \sum_n T_{fn}^\dagger \rho_n T_{ni}$$

■ Implications of **unitarity** constraint on transition matrix

1. Doesn't uniquely determine T_{ij} ; highly restrictive, however

Elastic: $\text{Im } (T^{-1})_{11} = -\rho_1$, $E < E_2$ (assuming T & P invariance)

Multichannel: $\text{Im } \mathbf{T}^{-1} = -\boldsymbol{\rho}$

2. Unitarity violating transformations

- Scaling single ampl: $T_{ij} \rightarrow \alpha_{ij} T_{ij} \quad \alpha_{ij} \in \mathbb{R}$

- Phase x-form: $T_{ij} \rightarrow e^{i\theta_{ij}} T_{ij} \quad \theta_{ij} \in \mathbb{R}$

★ consequence of linear ‘LHS’ \propto quadratic ‘RHS’

3. Unitary parametrizations of data provide constraints that experiment may violate

★ *normalization*, in particular

★ ^{17}O : Bair & Haas '73 vs. Harissopoulos '05

→ Observable \propto KF $|T_{fi}|^2$

- ENDF/B-VIII.0 release: *Nucl. Data Sheets 148 (2018) 1–142*



Theory

Unpolarized & polarized scattering/reaction observables

- Wolfenstein trace formalism
 - Spin density matrix

$$\langle O_f \rangle = \frac{\text{Tr } \rho_f O_f}{\text{Tr } \rho_f}$$

$$\rho_f = M \rho_i M^\dagger$$

$$M_{fi} = \frac{4\pi}{k_i} \langle s' m'_s | T | s m_s \rangle$$

$$\rho_i = \frac{1}{\text{Tr } \mathbb{1}_i} \sum_i \langle O_i \rangle O_i$$

$$\rho_i^{(0)} \equiv \frac{1}{N_s} \mathbb{1}_i$$

- Unpolarized

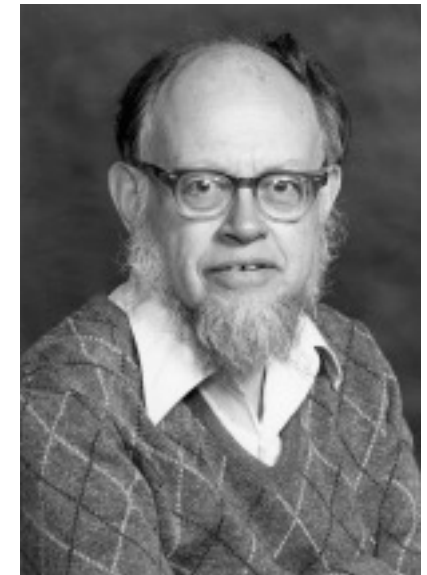
$$\text{Tr } \rho_i^{(0)} = \frac{1}{N_s} \text{Tr } M M^\dagger$$

$$\sigma^{(0)}(E, \theta) = \frac{4\pi}{k_i^2} \frac{1}{(2s_1 + 1)(2s_2 + 1)} \sum_{\{m_s\}} |\langle s' m'_s | \textcolor{blue}{T}(\{E_\lambda, \gamma_{\lambda,c}\}) | s m_s \rangle|^2$$

- General polarization

$$\sigma^{(0)}(E, \theta) \langle O_f \rangle = \frac{1}{\text{Tr } \mathbb{1}_i} \sum_i \langle O_i \rangle \text{Tr } M O_i M^\dagger O_f$$

$$\begin{cases} O_i = O_1 \otimes O_2 \\ O_f = O_3 \otimes O_4 \end{cases}$$



*Lincoln Wolfenstein
1923-2015*



R-matrix parametrization

Relativistic kinematics

$$R_{c'c}(E_\lambda, \gamma_{\lambda,c}) = \sum_\lambda \frac{\gamma_{\lambda,c'} \gamma_{\lambda,c}}{E_\lambda(s) - E(s)}$$

- Mandelstam s variable
 - Lorentz invariant
 - Channel invariant

$$p_{c,1}^\mu = (m_{c,1} + E_c, \mathbf{p}_{c,1}) \quad p_{c,2}^\mu = (m_{c,2}, 0)$$

$$s = (p_{c,1} + p_{c,2})^2 = m_c^2 + 2m_{c,2}E_c$$

$$m_c = m_{c,1} + m_{c,2}$$

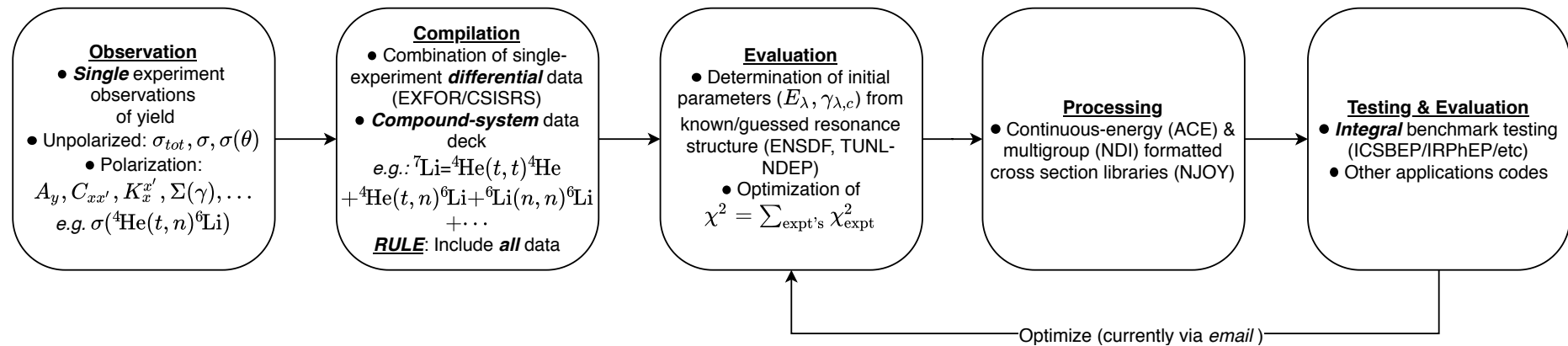
- Relativistic parametrization form (reference channel c_0)

$$E(s) = \frac{s - m_{c_0}^2}{2m_{c_0}}$$

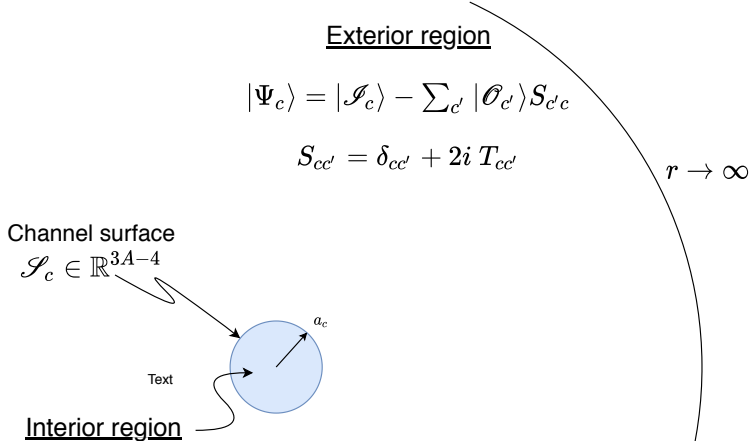


R-matrix evaluation for light nuclear systems

Nuclear Data Pipeline EDA cross section evaluation



- Cross section evaluation for light-elements ($A \leq 20$)
 - Quantum mechanical R-matrix (Wigner)
 - Correlates **all** experimental data simultaneously
 - pol/unpol; neutrons/charged-particles
 - Elastic/inel/transfer/reaction/break-up
 - Upper energy-limit restricted (break-up) < 20 MeV



$$[H + \mathcal{L}_B] |\lambda\rangle = E_\lambda |\lambda\rangle$$

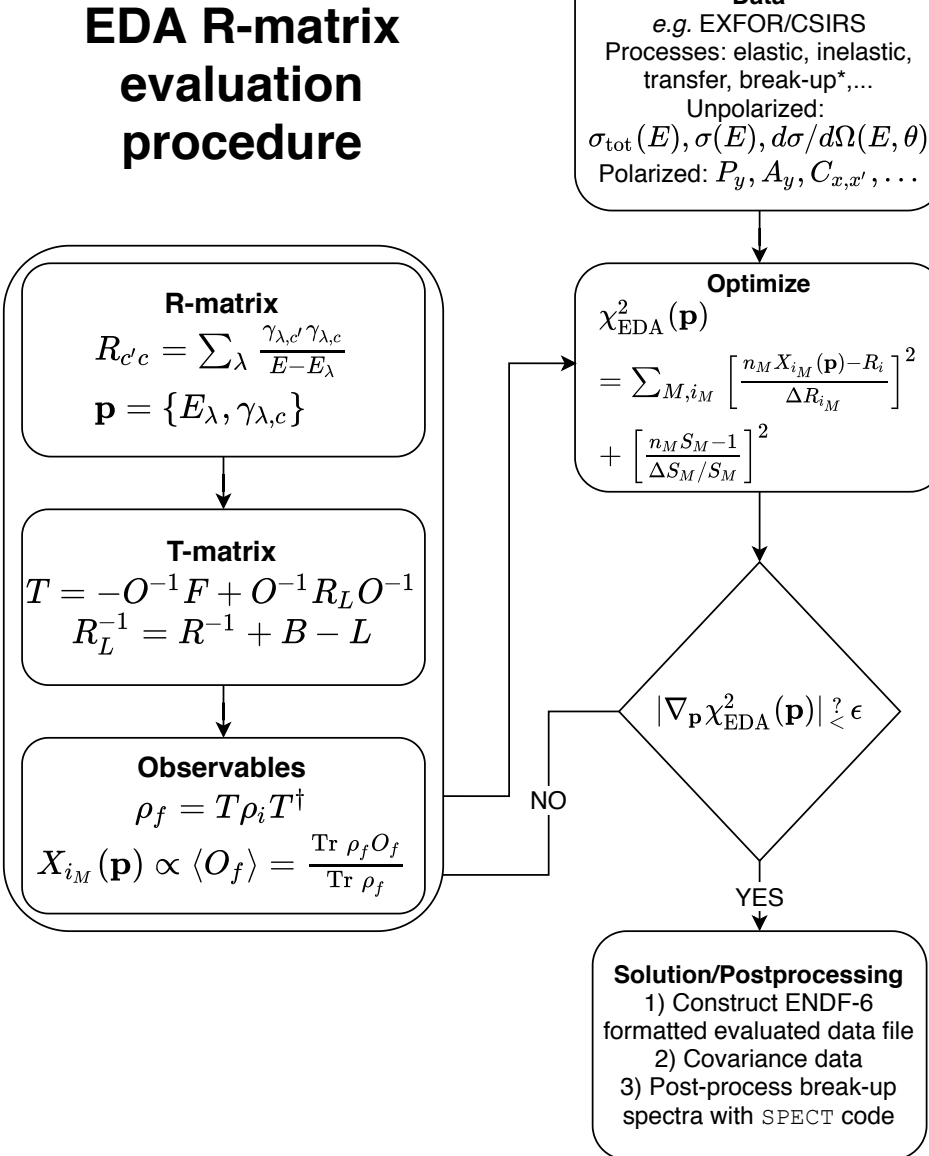
$$|\Psi\rangle = [H + \mathcal{L}_B - E]^{-1} \mathcal{L}_B |\Psi\rangle$$

$$\mathcal{L}_B = \sum_c \frac{ia_c}{2m_c} |a_c\rangle \langle a_c| (\hat{p}_r + iB_c)$$

$$R_{B,c'c} = \langle c' | [H + \mathcal{L}_B - E]^{-1} | c \rangle = \sum_\lambda \frac{\langle c' | \lambda \rangle \langle \lambda | c \rangle}{E_\lambda - E}$$



EDA evaluation procedure



Parameter uncertainty from χ^2

The Old Way gives too-small uncertainty

- At a solution: $\left. \frac{\partial \chi^2}{\partial p} \right|_{\hat{p}} \approx 0 \quad \chi^2(p) \approx \chi^2(\hat{p}) + \sum_{\alpha, \beta=1}^{N_p} \delta p_\alpha (C^{-1})_{\alpha\beta} \delta p_\beta$
- Variations at \hat{p} : $\delta \chi^2(p) = \chi^2(\hat{p} + \delta p) - \chi^2(\hat{p})$
 $= \delta p_1 A \delta p_1 + \delta p_1 B \delta p_2 + \delta p_2 B^T \delta p_1 + \delta p_2 D \delta p_2$

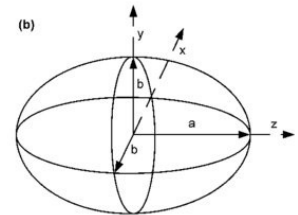
- Change in χ^2 when $\{p_2\}$ change, re-optimize $\delta \chi^2$ w.r.t. $\{p_1\}$

$$\delta \chi^2(p_1 + \delta p_1^{min}, p_2 + \delta p_2) = \sum_{\alpha, \beta=N_1+1}^{N_2} \delta p_{2,\alpha} \tilde{D}_{\alpha\beta}^{-1} \delta p_{2,\beta}$$

- \tilde{D} : restriction of C to $\{p_2\}$ -subspace

$$\delta \chi^2 = \frac{(\delta p_0)^2}{C_{00}} \implies \delta p_0 = (C_{00})^{1/2} \iff \delta \chi^2 = 1$$

- NB: the $\delta \chi^2 = 1$ hypersurface's average distance shrinks with incr. N_p



Parameter variance

- At a solution $\left. \frac{\partial \chi^2}{\partial p} \right|_{\hat{p}} \approx 0 \quad \chi^2(p) \approx \chi^2(\hat{p}) + \sum_{\alpha, \beta=1}^{N_p} \delta p_\alpha (C^{-1})_{\alpha\beta} \delta p_\beta$
- Assuming a normal distribution

$$P_c(p|y) = \frac{1}{\det C^{1/2} (2\pi)^{N_p/2}} e^{-\frac{1}{2} [\chi^2(p) - \chi^2(\hat{p})]},$$

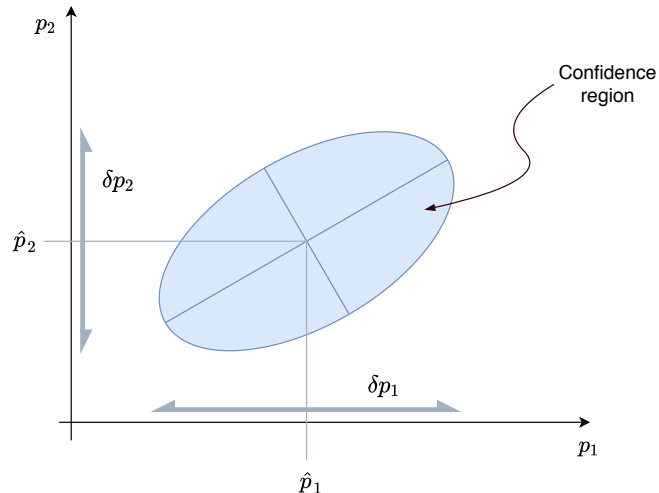
$$\langle (\delta p_\alpha)^2 \rangle = \int_{-\infty}^{\infty} dp_1 \cdots \int_{-\infty}^{\infty} dp_{N_p} P_c(p|y) (\delta p_\alpha)^2 = C_{\alpha\alpha}$$

- Change in chi-squared $\delta p_\mu = (C_{\alpha\alpha})^{1/2} \delta_{\mu\alpha}$

$$\delta \chi^2(p) = \chi^2(\hat{p} + \delta p) - \chi^2(\hat{p}) = \sum_{\alpha, \beta} \delta p_\alpha (C^{-1})_{\alpha\beta} \delta p_\beta$$

$$\delta \chi^2(\delta p_\mu) = C_{\mu\mu} C_{\mu\mu}^{-1} = 1 - \sum_{\beta \neq \mu} (C_{\mu\beta})^2 < 1$$

- NB: adding redundant params can lower $\delta \chi^2(\delta p_\mu)$



Uncertainties from chi-squared minimization

$$\chi^2_{\text{EDA}}(\mathbf{p}) = \sum_{M,i_M} \left[\frac{n_{i_M} X_{i_M}(\mathbf{p}) - R_{i_M}}{\delta R_{i_M}} \right]^2 + \left[\frac{n_M S_M - 1}{\delta S_M / S_M} \right]^2 \quad \left\{ \begin{array}{l} M : \text{experimental setup} \\ i : \text{observable} \\ R_{i_M}, \delta R_{i_M} : \text{relative measurement, uncert.} \\ X_{i_M} : \text{calc'd observable} \\ n_M : \text{normalization} \end{array} \right.$$

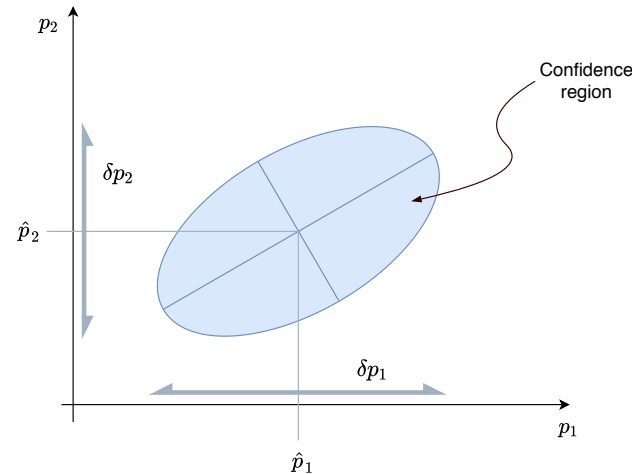
Uncertainty determination comparison:

1) previous: $\delta\chi^2 = 1 \implies$ Uncertainties too small; scaling: $\delta p_i = (C_{ii}^0)^{1/2} \sim \mathcal{O}(N_p^{-1/2})$

2) improved:

$$P(\delta\chi^2 | k \text{ DOF}) = \frac{1}{2^{k/2}\Gamma(k/2)} \int_0^{\delta\chi^2} dt t^{k/2-1} e^{-t/2} = \text{CL}(68\%: 1-\sigma; 95\%: 2-\sigma; \dots)$$

Better scaling: $\delta p_i \sim (N_p C_{ii})^{1/2}$



Observable error propagation

Covariance matrix

The parameter covariance matrix is $\mathbf{C}_0 = 2\mathbf{G}_0^{-1}$, and so first-order error propagation gives for the cross-section covariances

$$\begin{aligned}\chi^2(\mathbf{p}) &= \chi_0^2 + (\mathbf{p} - \mathbf{p}_0)^T \mathbf{g}_0 + \frac{1}{2}(\mathbf{p} - \mathbf{p}_0)^T \mathbf{G}_0(\mathbf{p} - \mathbf{p}_0) \\ &= \chi_0^2 + \Delta\chi^2.\end{aligned}\quad \left\{ \begin{array}{l} \chi_0^2 = \chi^2(\mathbf{p}_0) \\ \mathbf{g}_0 = \nabla_{\mathbf{p}}\chi^2(\mathbf{p}) \Big|_{\mathbf{p}=\mathbf{p}_0} \approx 0 \\ \mathbf{G}_0 = \nabla_{\mathbf{p}}\mathbf{g}(\mathbf{p}) \Big|_{\mathbf{p}=\mathbf{p}_0} \end{array} \right.$$

$$\begin{aligned}\text{cov}[\sigma_i(E)\sigma_j(E')] &= \left[\nabla_{\mathbf{p}}\sigma_i(E) \right]^T \mathbf{C}_0 \left[\nabla_{\mathbf{p}}\sigma_j(E') \right] \Big|_{\mathbf{p}=\mathbf{p}_0} \\ &= \Delta\sigma_i(E)\Delta\sigma_j(E')\rho_{ij}(E, E').\end{aligned}$$

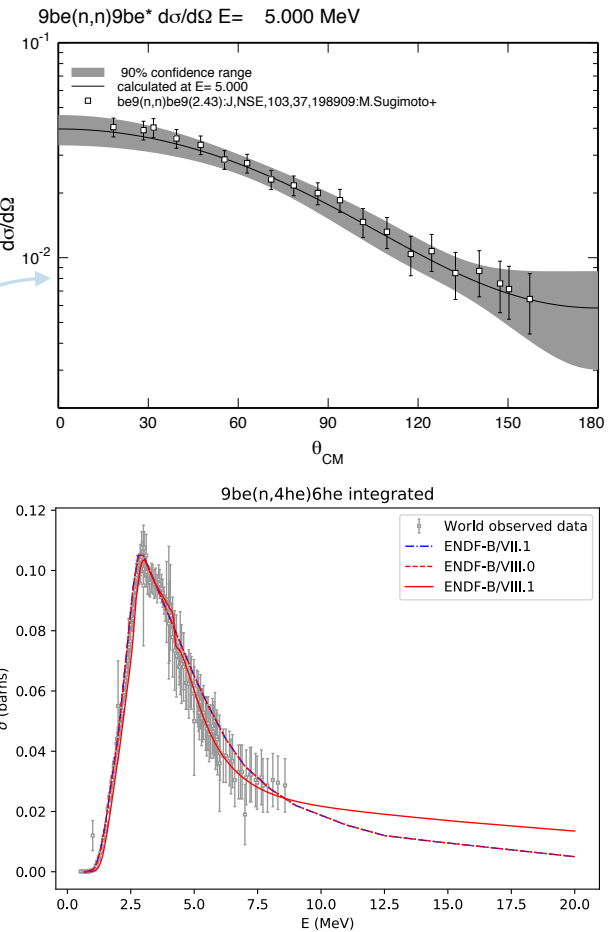
observable uncertainties

correlation coefficient



New code implementation

- Previous version **EDA5**
 - Versatile, numerically stable; legacy [F66 remnants] → difficult to modify/debug
- Current version **EDAf90**
 - **ModernFORTRAN (F90)** implementation
 - Identical numerically to **EDA5**
 - Interfaces with **NJOY2016/NJOY21**
 - Backend interface with **ENDFtk**
 - Frontend (observed data) interface with EXFOR/CSISRS (**c5** format)



Charge-Independent Analysis of N-N Scattering up to 50 MeV

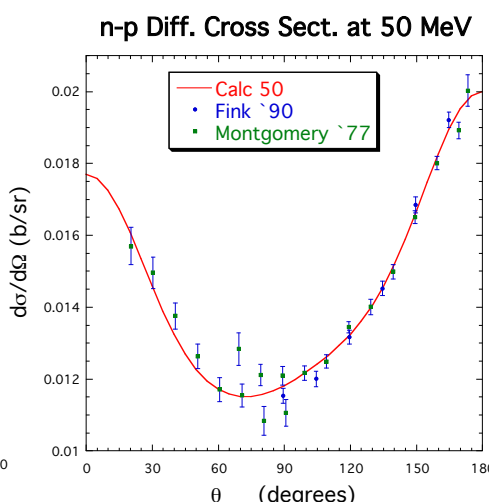
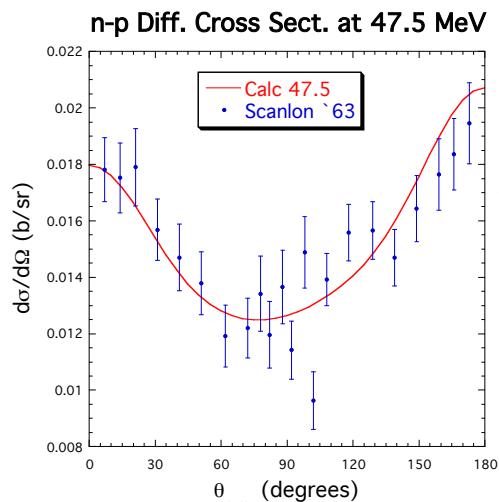
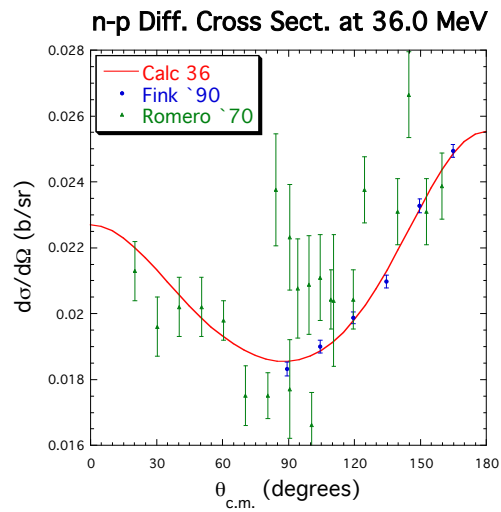
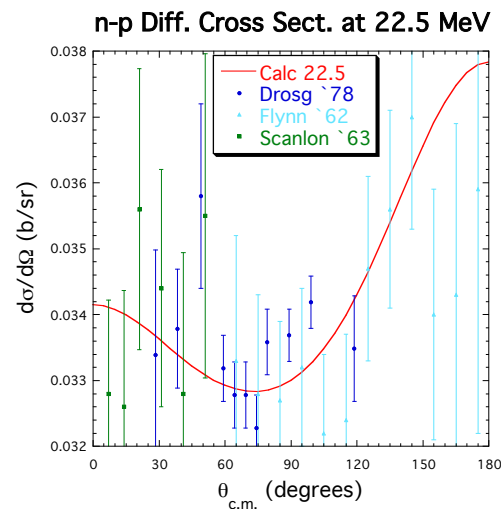
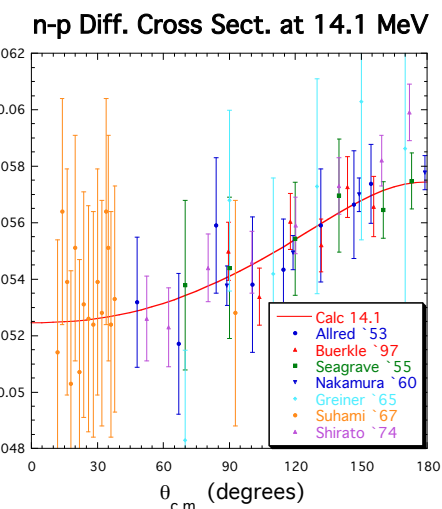
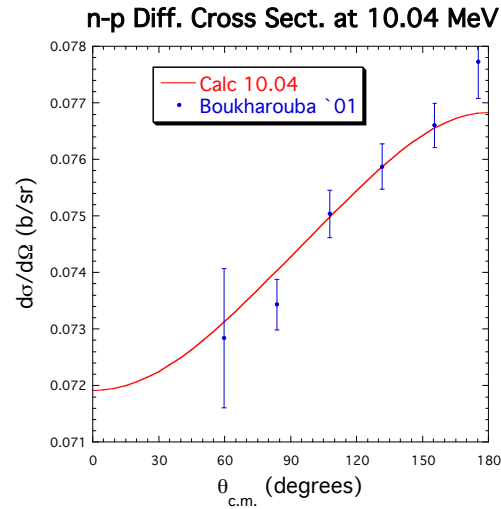
Channel	σ_c (fm)	I_{\max}
p+p	3.26	3
n+p	3.26	3
$\gamma+d$	40	1
n+n	3.26	3

Reaction	# Pts.	χ^2	Observable Types
p(p,p)p	675	950	$\sigma(\theta), A_y(p), C_{x,x}, C_{y,y}, K_x^{x'}, K_y^{y'}, K_z^{x'}$
p(n,n)p	4815	3764	$\sigma_T, \sigma(\theta), A_y(n), C_{y,y}, K_y^{y'}$
p(n, γ)d	86	179	$\sigma_{int}, \sigma(\theta), A_y(n)$
d(γ ,n)p	88	77	$\sigma_{int}, \sigma(\theta), \Sigma(\gamma), P_y(n)$
n(n,n)n	1	0	a_0
Norms.	183	86	
Total	5848	5056	20

free parameters = 43+183 $\Rightarrow \chi^2/\text{degree of freedom} = 0.899$

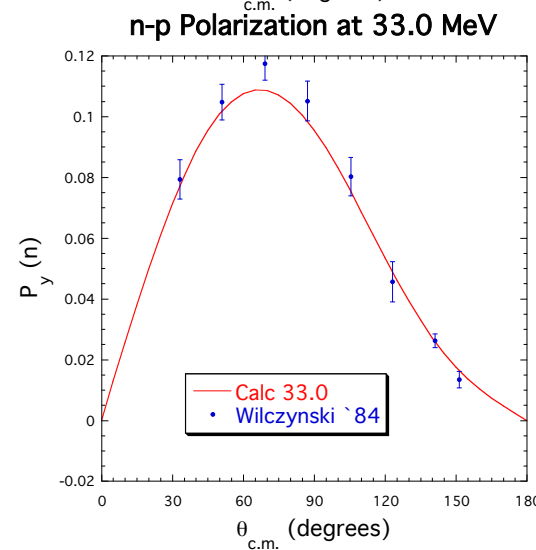
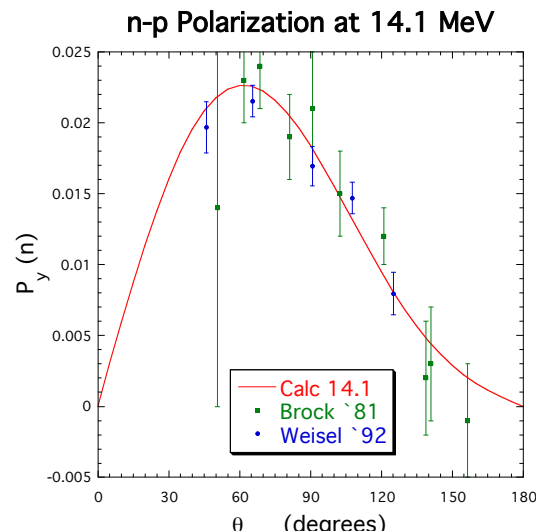
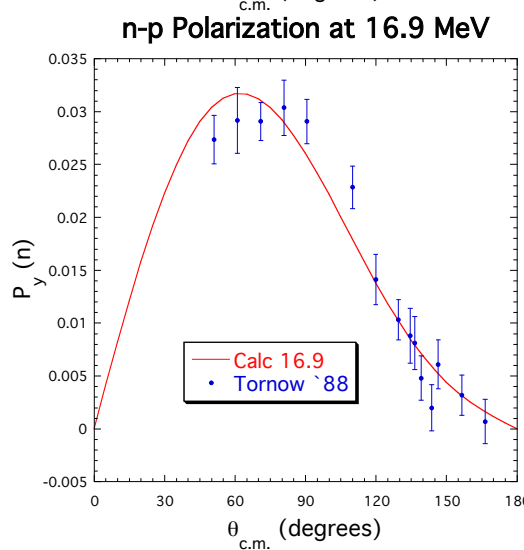
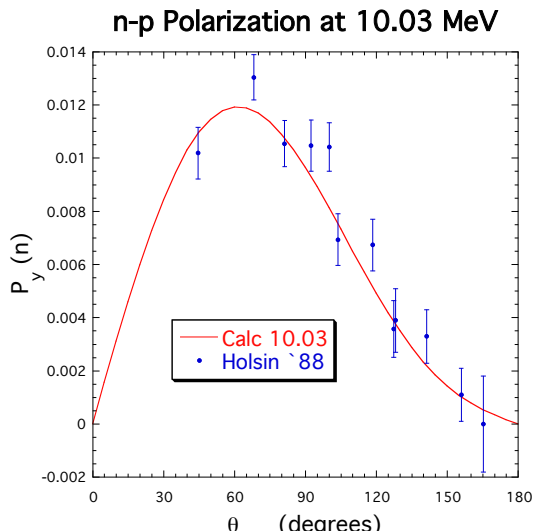


n-p Elastic Scattering Differential Cross Sections

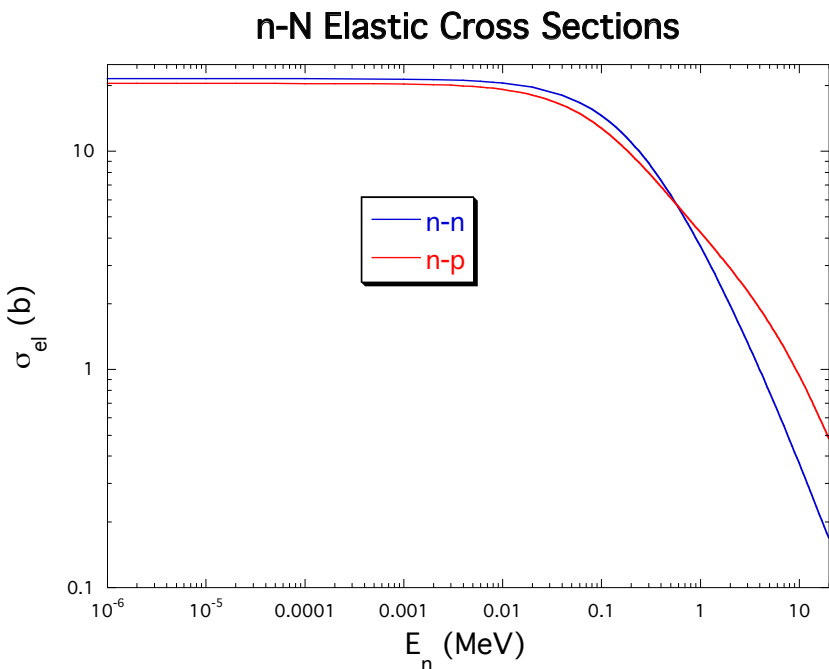
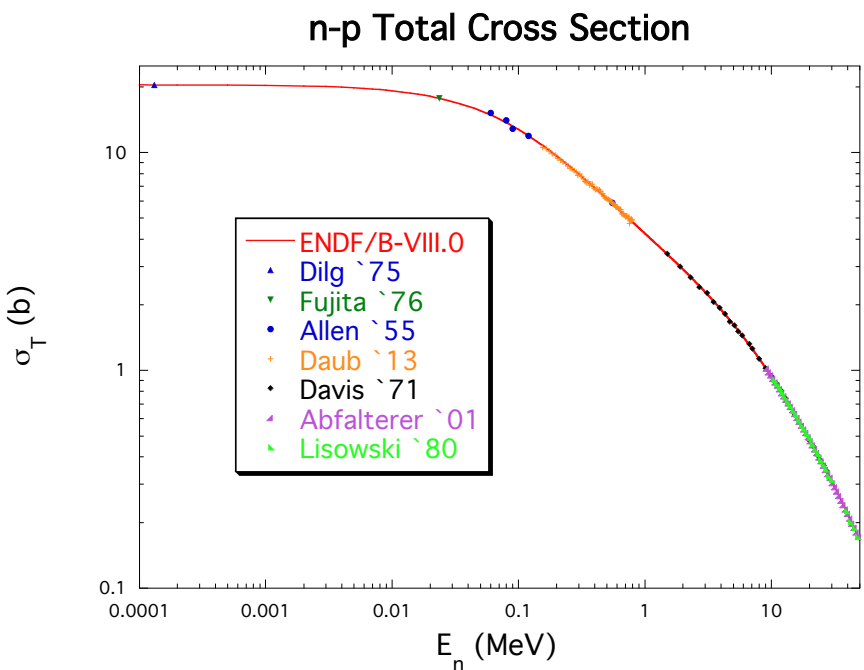


n-p Elastic Scattering Polarizations

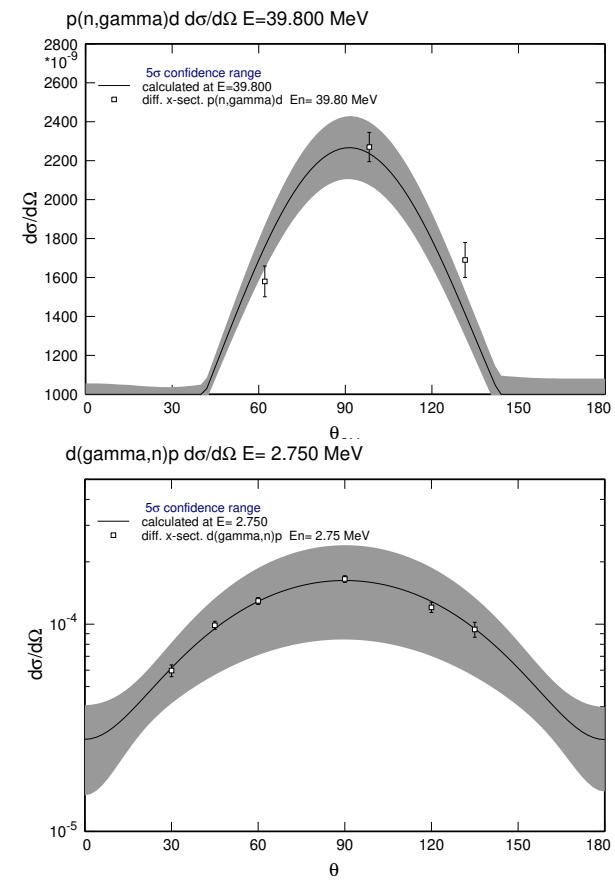
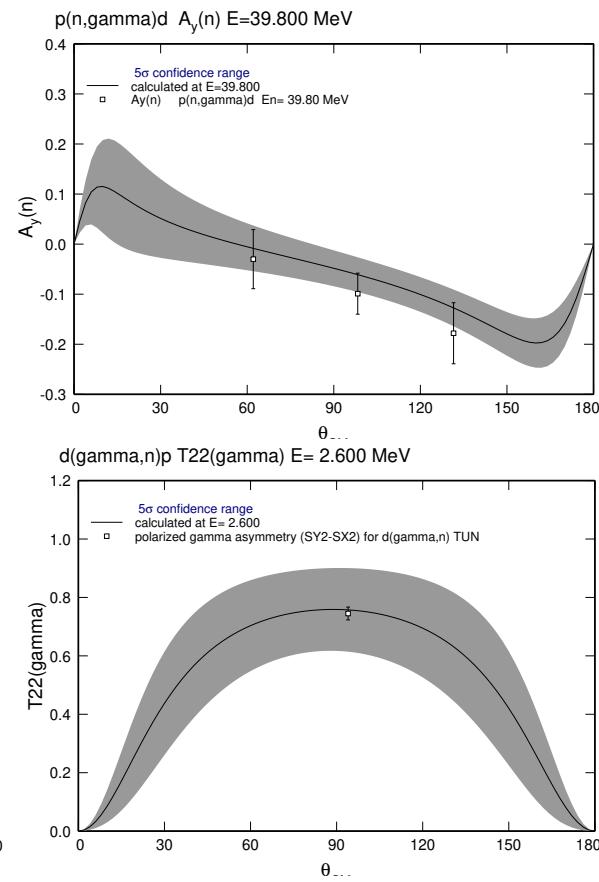
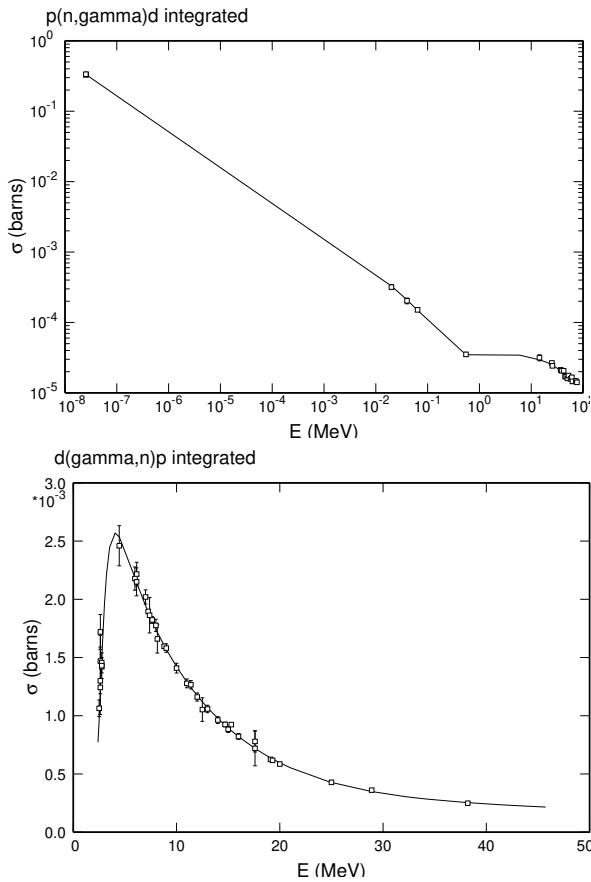
- Why include polarizations?
- Further constrain the scattering amplitudes and possibly find a unique solution (χ^2 minimum).



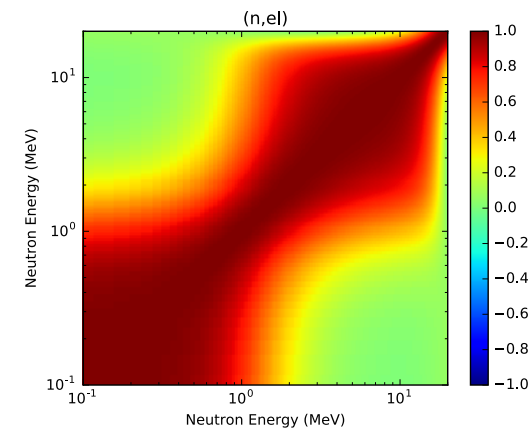
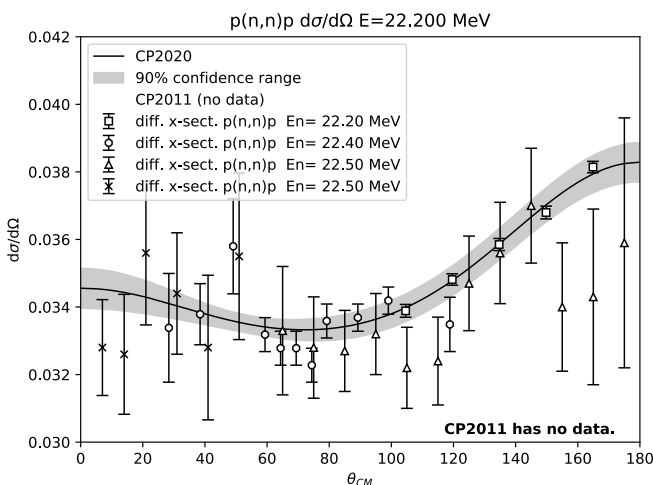
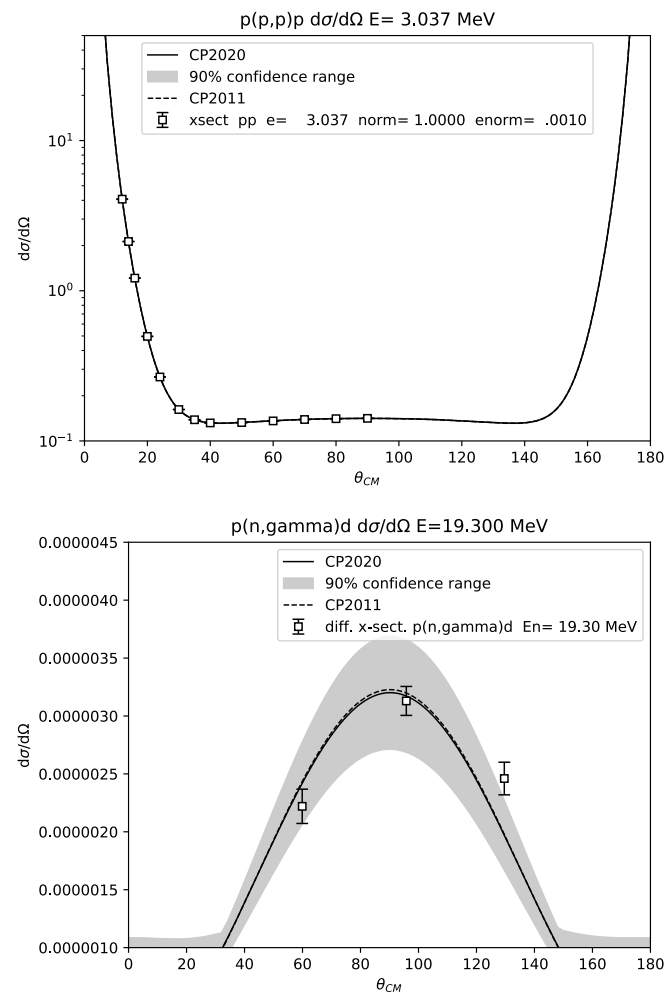
Integrated Cross Sections for n-p and n-n Scattering



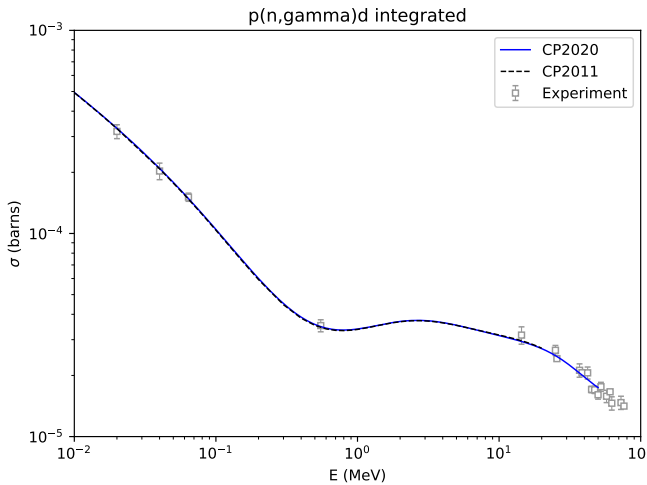
n+p Capture and g+d Photodisintegration Data



NN system covariance data



Covariance matrix



Partitions:
 $pp(\ell \leq 3); np(\ell \leq 3);$
 $\gamma d(\ell \leq 1); nn(\ell \leq 3)$

36 channels ($J^\pi LS$)

$$\chi^2/\text{dof} \simeq 0.9$$



R-matrix evaluation

^5Li system

Channel	a_c (fm)	l_{max}
$d + ^3\text{He}(\frac{1}{2}^+)$	4.8	4
$p + ^4\text{He}(0^+)$	2.9	4
$p + ^4\text{He}^*(0^+; 20.2 \text{ MeV})$	3.4	2
$d_0 + ^3\text{He}(\frac{1}{2}^+)$	5.1	0

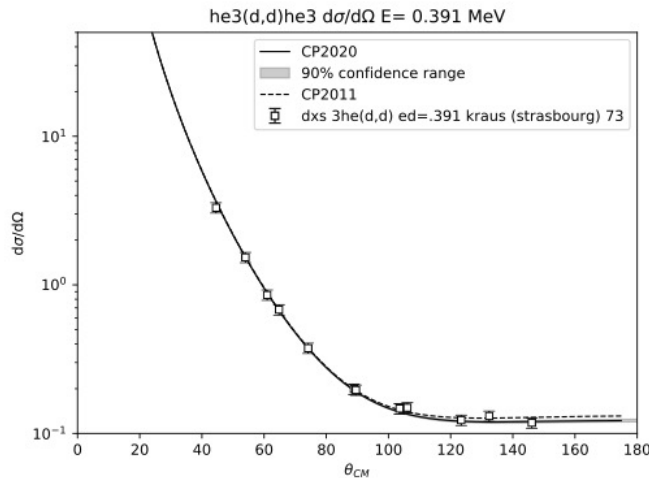
Reaction	Energy Range (MeV)	# Data Points	Observables
$^3\text{He}(d, d)^3\text{He}$	$E_d = 0.32 - 10.0$	2,229	$\sigma(\theta), A_i, A_{ii}, C_{i,j}, C_{ij,k}, K_{i,j'k'}, K_{ij,k'l'}$
$^3\text{He}(d, p)^4\text{He}$	$E_d = 0.13 - 10.0$	3,839	$\sigma(E), \sigma(\theta), A_i, A_{ii}, C_{i,j}, K_{ij,k'}$
$^3\text{He}(d, p)^4\text{He}^*$	$E_d = 3.70 - 6.70$	28	$\sigma(\theta)$
$^4\text{He}(p, p)^4\text{He}$	$E_p = 0.92 - 34.3$	867	$\sigma(E), \sigma(\theta), A_y, P_y$
	Total:	6963	

Table 1: Channel configuration (top) and data summary (bottom) for the ^5Li system analysis. The column labeled “Observables” indicates the following data types: $\sigma(E)$, integrated cross section; $\sigma(\theta)$, unpolarized angular distributions (energy-dependence suppressed); A initial-state analyzing power; P final-state polarization; C spin correlation coefficients; K polarization transfer coefficients. (We have suppressed the indices i, j, \dots which take on values x, y, z for spins/polarization directions in configuration space.) All polarization and spin distributions are angular distributions, which depend on the angle of the outgoing particle. Chi-squared per degree of freedom for the analysis is $\chi^2/\text{dof} \simeq 2.7$ over 7,178 data points, 215 of which were discarded by eliminating individual data points which contribute to $\chi^2 > 40$.

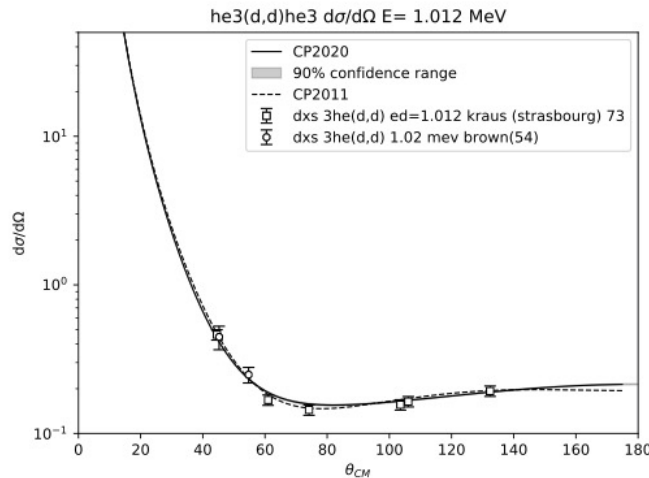


⁵Li system evaluation

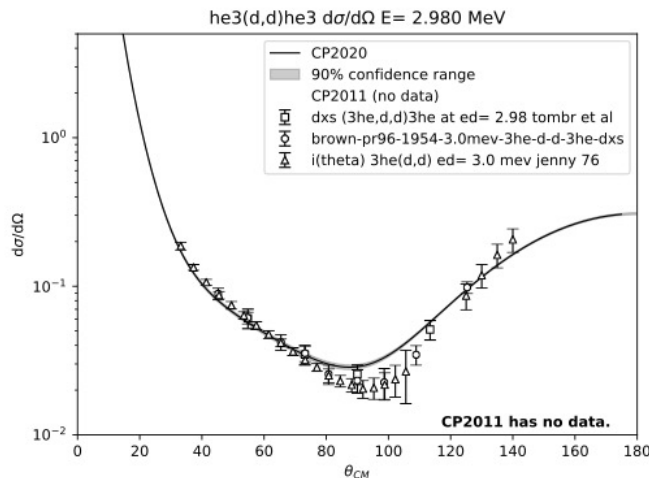
³He(d,d)³He



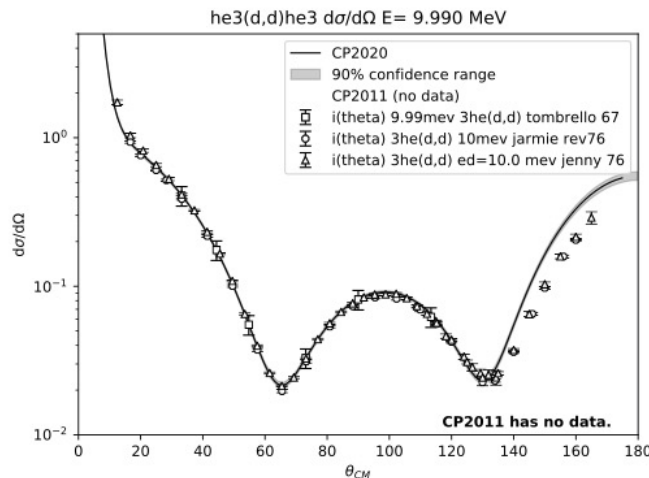
(a)



(b)



(c)

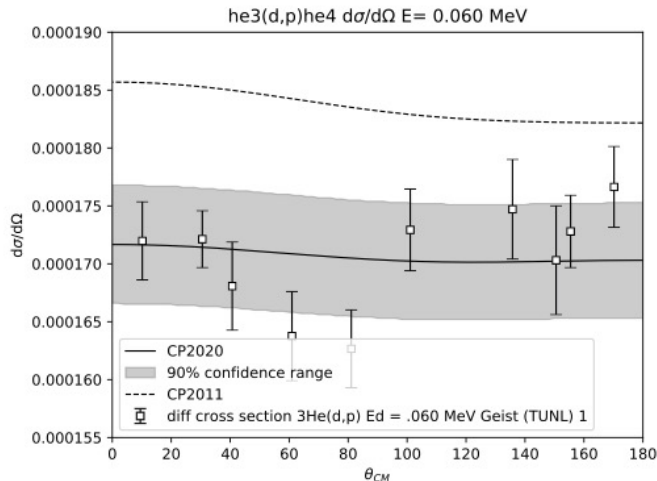


(d)

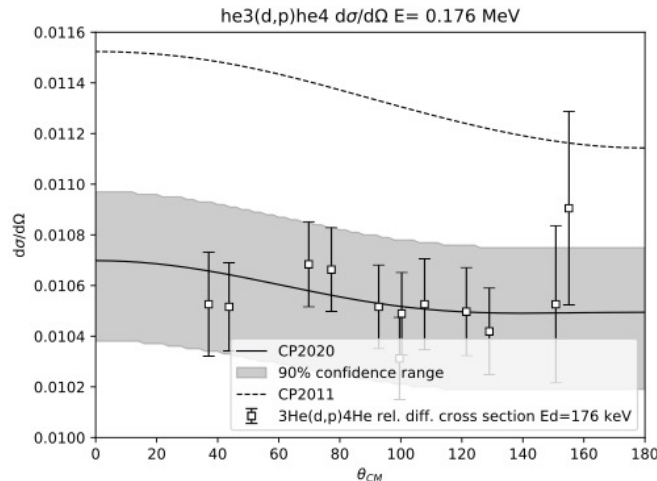


^5Li system evaluation

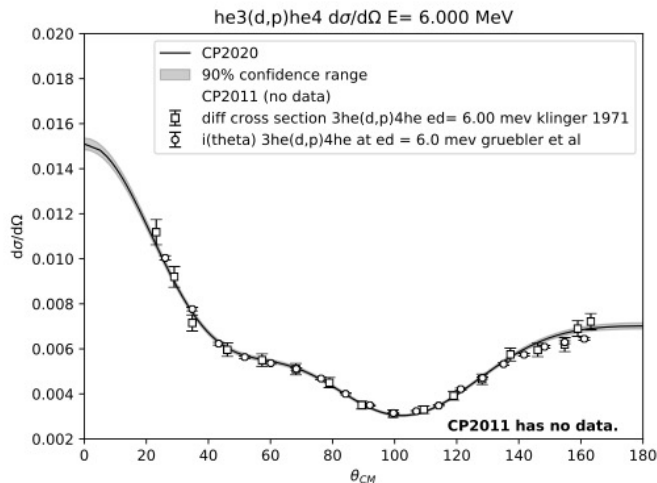
$^3\text{He}(\text{d},\text{p})^4\text{He}$



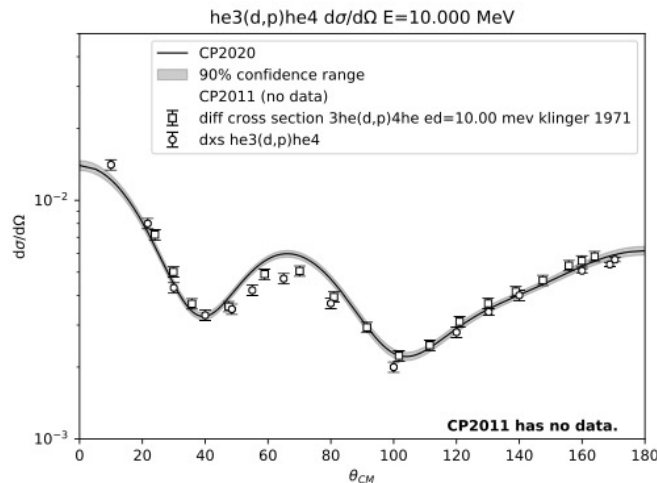
(a)



(b)



(c)

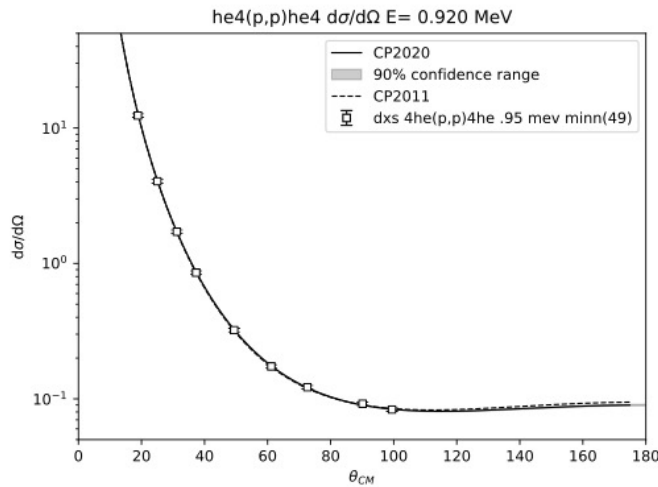


(d)

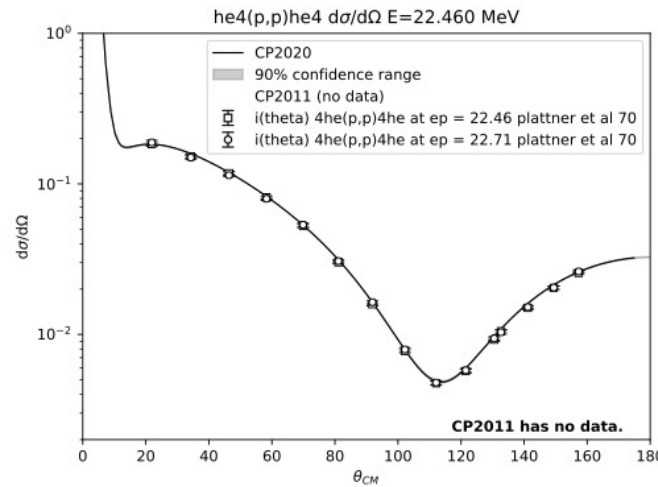


^5Li system evaluation

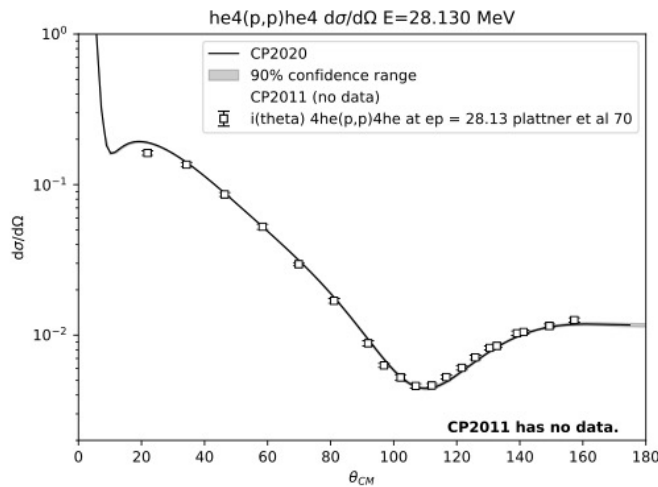
$^4\text{He}(\text{p},\text{p})^4\text{He}$



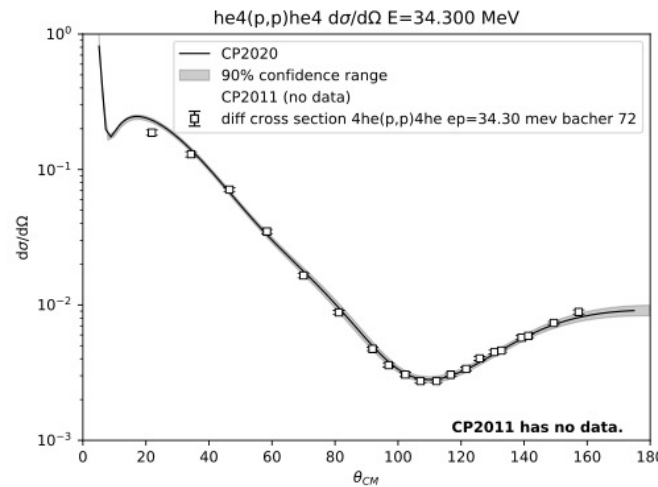
(a)



(b)



(c)



(d)



$n+{}^9\text{Be}$

New evaluation

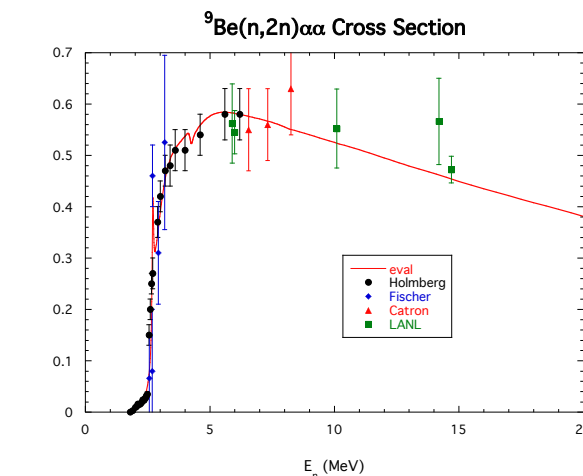
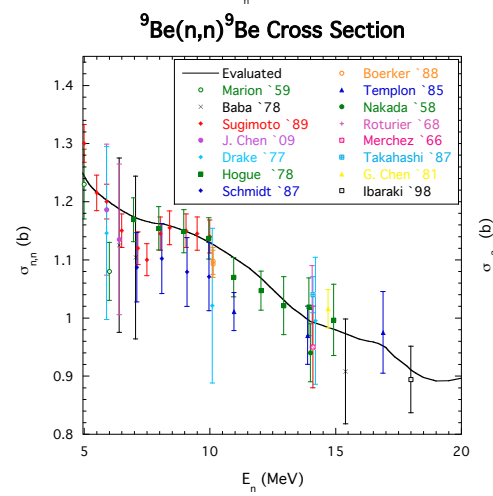
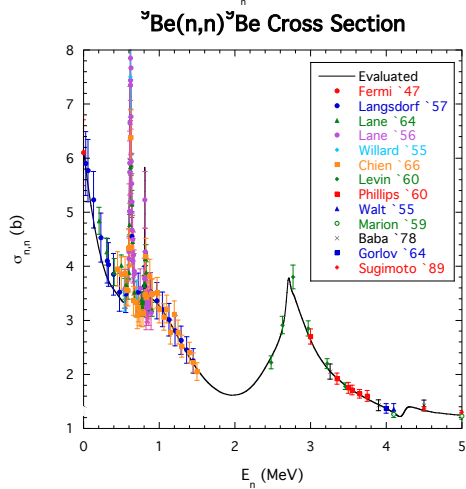
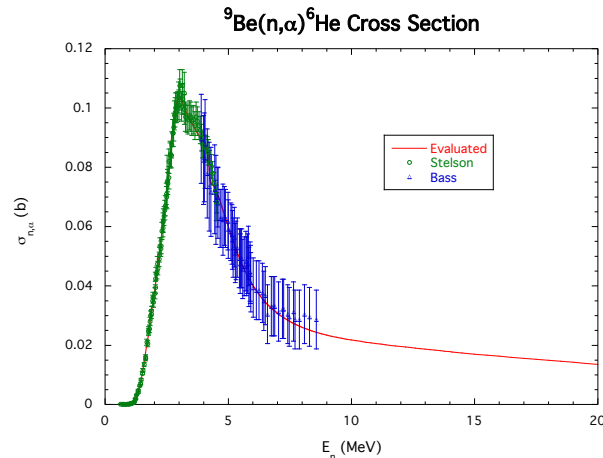
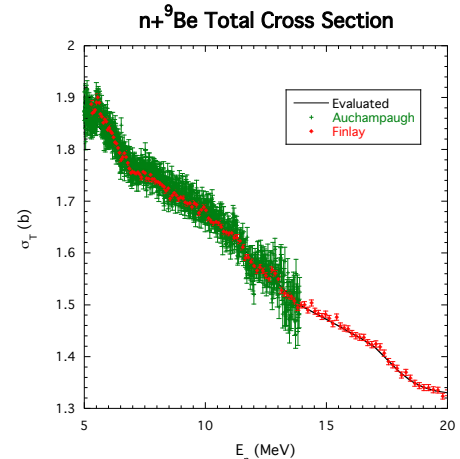
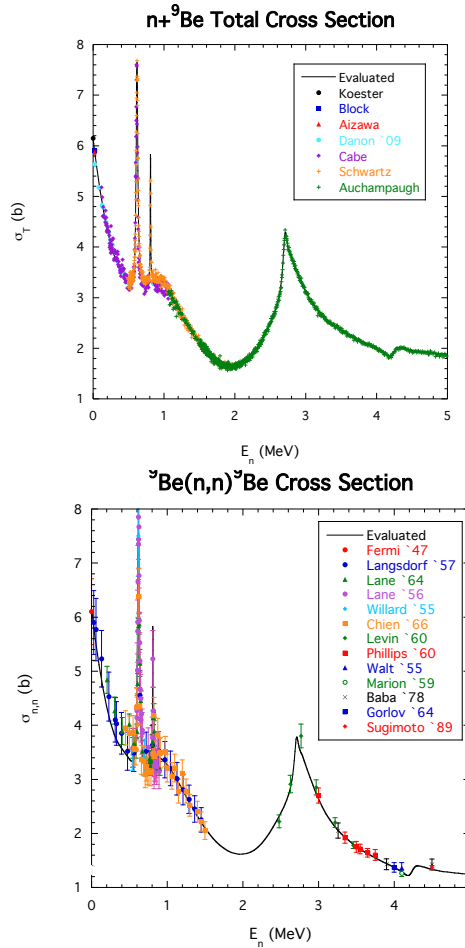
- Added data: elastic, (n,α) , (n,n_1)

Channel	$a_c(\text{fm})$	ℓ_{\max}
$n+{}^9\text{Be}(\frac{3}{2}^-)$	4.67	3
${}^4\text{He}+{}^6\text{He}(0^+)$	5.00	4
$(nn)_0+{}^8\text{Be}(2^+)$	5.20	3
$n+{}^9\text{Be}^*(\frac{5}{2}^-)$	5.20	1

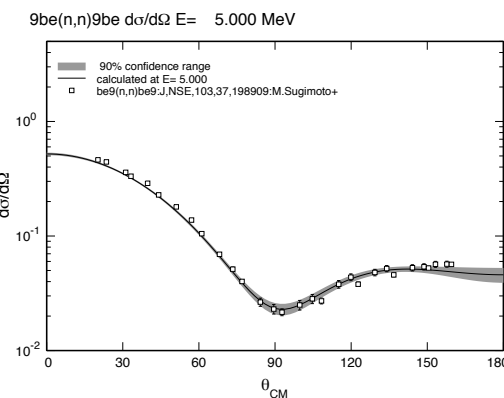
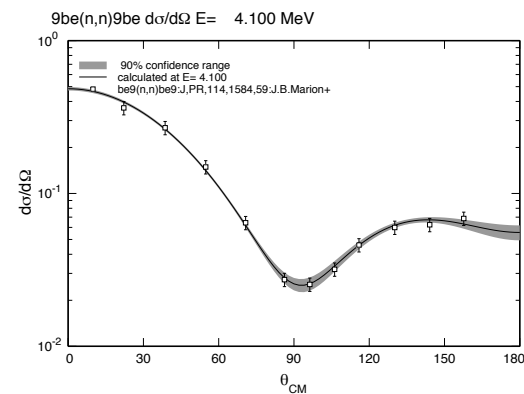
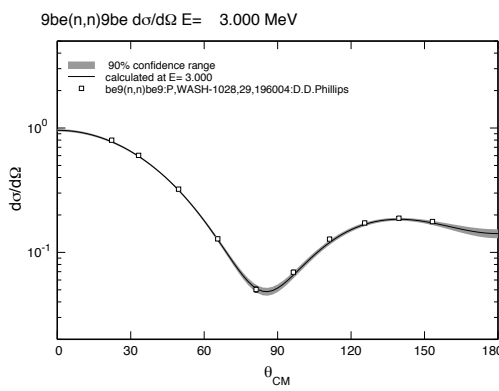
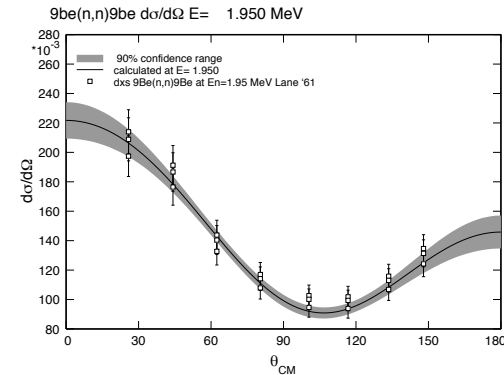
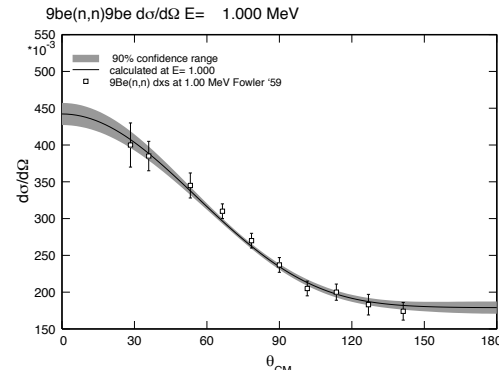
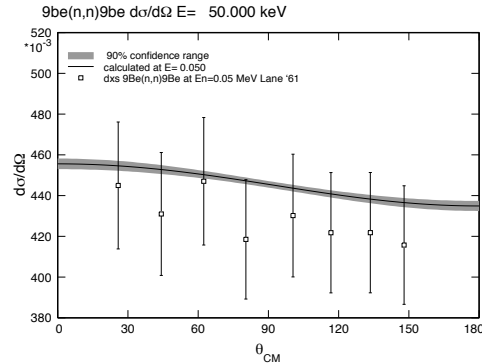
Process	E_n range	Observables	N_{dat}	χ^2/N_{dat}
${}^9\text{Be}(n, n_0){}^9\text{Be}$	(1.25 eV, 15.4 MeV)	$\sigma_{\text{tot}}, \sigma, \sigma(\theta), A_y(\theta)$	5782	1.65
${}^9\text{Be}(n, {}^4\text{He}){}^6\text{He}$	(0.63, 8.5) MeV	$\sigma, \sigma(\theta)$	178	1.40
${}^9\text{Be}(n, 2n){}^8\text{Be}$	(1.8, 14.7) MeV	σ	40	NA
${}^9\text{Be}(n, n_1){}^9\text{Be}^*$	(2.7, 5.0) MeV	$\sigma(\theta)$	83	1.65
Total			6083	1.75



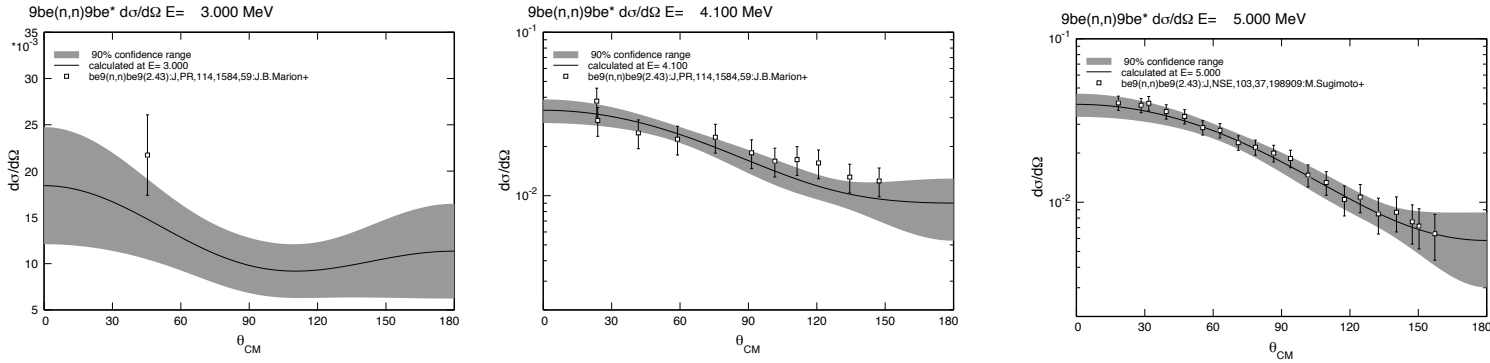
$n+{}^9\text{Be}$ Integrated Cross Sections



${}^9\text{Be}(n,n){}^9\text{Be}$ Differential Cross Sections



${}^9\text{Be}(n,n_2){}^9\text{Be}^*$ Differential Cross Sections

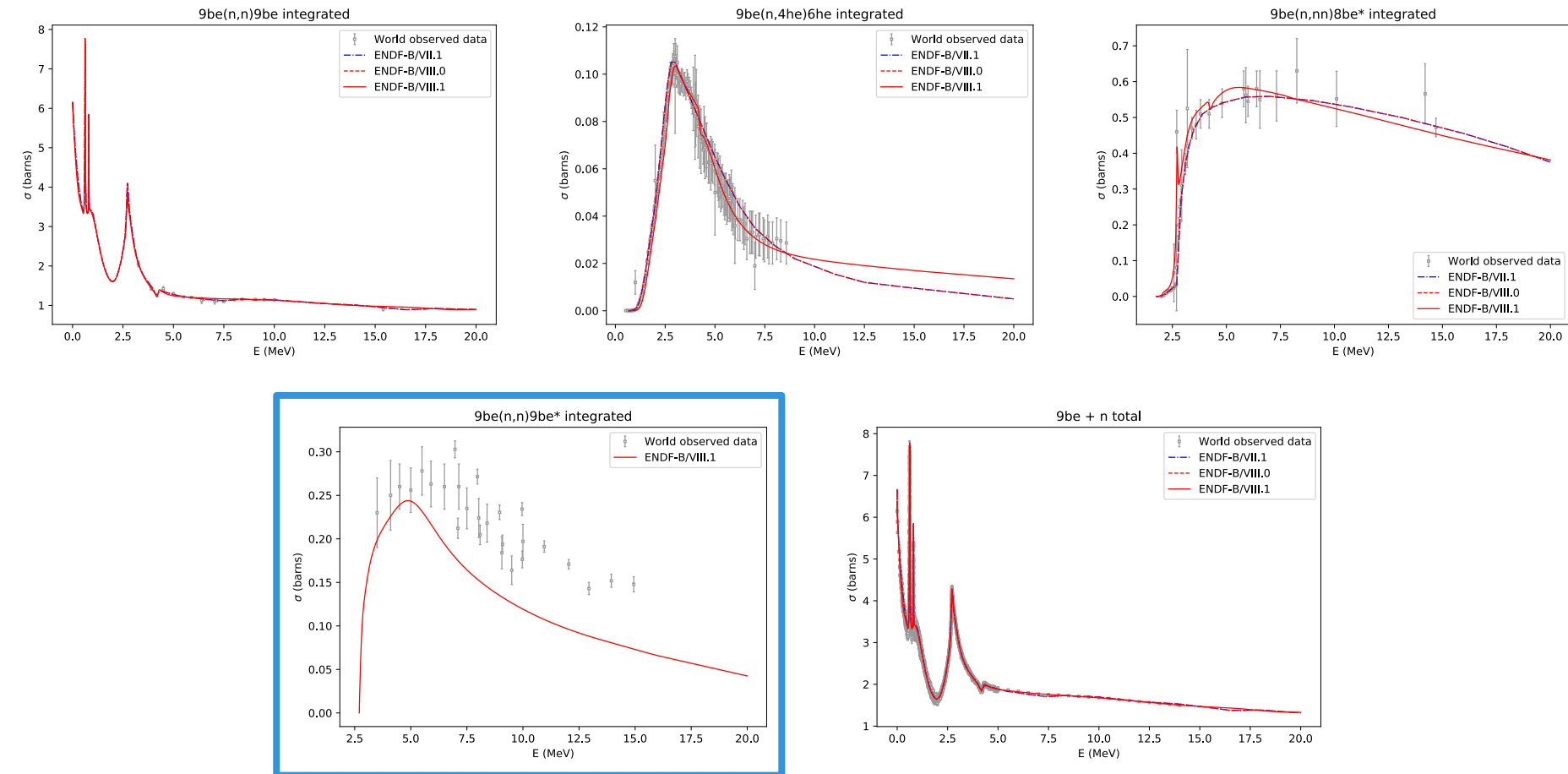


Summary of new evaluation:

- ${}^{10}\text{Be}$ analysis has produced a consistent set of cross sections and angular distributions that are in agreement with most of the experimental data at energies up to 5 MeV. Extensions above that energy were based on the experimental data alone.
- Level assignments for the overlapping resonances near $E_n=2.7$ MeV have the opposite parity ($4^-, 3^+ \rightarrow 4^+, 3^-$).
- Excited states of ${}^9\text{Be}$ make important contributions to the $(n,2n)$ cross section (MT=16 \rightarrow 24 in the new evaluation).
- Testing/benchmarking: (M. Herman, LANL) and thick-target angular neutron yields (Y. Danon, RPI) on the following slides



Comparison to previous ENDF/B Integrated cross sections



Conclusions

- R-matrix
 - Correlates all processes associated with a given compound system
 - Enforces
 - Unitarity, relating the *magnitudes* and *phases* of amplitudes of different processes (total, elastic, inelastic, reaction, etc.)
 - Causality; proper complex-analytic properties
- Systematically improvable
 - More data
 - Polarized observables
 - Higher-energy data



Outlook

- Continued code modernization & improvement
 - Higher energies → break-up reactions
 - Currently post-processed by auxiliary codes
 - Immediate objective: $(z,z'n)$, $(z,z'\gamma)$, etc.
- Uncertainty quantification
 - Currently
 - χ^2 minimization with per-experimental setup normalization
 - Appears sufficient for 2 \rightarrow 2 body scattering/reactions, single compound system
 - Planned
 - Bayesian statistical methods
 - Data covariances
 - Several compound systems concurrently
- Ongoing/planned evaluation
 - ${}^9\text{Be}$, ${}^{17}\text{O}$
 - Neutrons on H,C,N,O

Thank you for your patience and attention.

